THE JOURNAL OF PHYSICAL CHEMISTRY B

ARTICLE

pubs.acs.org/JPCB

Atomistic Simulations of Electroporation in Water Preembedded Membranes

Sheng Sun,[†,‡] Joseph T. Y. Wong,[§] and Tong-Yi Zhang*[,∥]

[†]Bioengineering Graduate Program, [§]Division of Life Science, and [∥]Department of Mechanical Engineering, The Hong Kong University of Science and Technology, Hong Kong, China SAR

[‡]Department of Engineering Mechanics, School of Mechanics and Materials, Hohai University, Nanjing 210098, China

Supporting Information

ABSTRACT: Atomistic simulations of electroporation were conducted on water/membrane/water systems, in which the membranes initially contained randomly distributed water molecules that might be introduced by acoustic treatment. The simulation results indicate that the critical strength of an applied electric field to induce electroporation is greatly reduced due to the initially embedded water molecules in the membranes. A lower applied electric field will significantly enhance the viability of cells in electroporation.

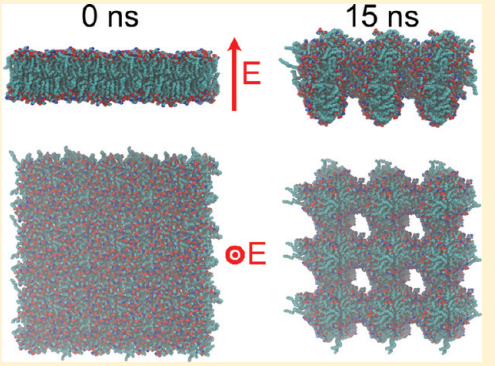

INTRODUCTION

Cell membrane provides a barrier against substance exchange between the inside and the outside of a cell, thereby allowing the cell to maintain its delicate internal contents. The main compositions of biomembranes are amphiphilic phospholipids, which form various ordered microstructures in water via self-assembly. The hydrophobic tails of membranes are buried inside the microstructures, and the polar hydrophilic headgroups are contacted with water. Because the aggregation force of lipids is weak, the microstructures of membranes can be changed by using external fields. Applying ultrasound or electric field can produce water holes through the membranes, and the techniques are termed sonoporation and electroporation, respectively.[1,2] Sonoporation and electroporation have been widely used in DNA cloning to transfer plasmid DNA into target cells.[3] They have the advantage of nonimmunogenicity and noninvasion. The critical transmembrane electric voltage is about 0.5−1.5 V to induce electroporation[4] and electrofusion.[5] If the applied electric field is too high, it will damage and kill the cells.[6] Under ultrasound treatment, water molecules permeate into the membrane and form water holes.[7] In molecular dynamics (MD) simulations,[8,9] water molecules could be initially and randomly introduced into the hydrophobic region of biomembranes. MD simulations on water-containing membranes show the dynamic process, at the atomic scale, of the self-aggregation of preembedded water molecules and the formation and evolution of water holes.[10]

The electroporation mechanism of biomembranes without preembedded water has been studied extensively by MD simulations,[11−16] indicating that the driving force to form water holes is the local electric field gradient at water/membrane interfaces which is induced by the reorientation of water dipoles under an external electric field. Since the time for electropore formation is exponentially related to the electric field strength,[11,16] the minimal field of electroporation obtained from MD simulations may be different if the simulation cutoff time is different. Thus, a proper cutoff of simulation time must be chosen to determine the minimal field from MD simulations.[16] With the cutoff time of 25 ns, the determined minimal field ranges from 0.26 to 0.38 V/nm, varying from one membrane to another membrane.[16] In the present work, we take this 25 ns cutoff simulation time to investigate the minimal field for electroporation.

Electroporation is efficient in therapy and gene transfection. However, an applied electric field may kill or damage cells if its strength is too high. To reduce any potential damage in electroporation, an applied electric field should be as weak as possible. One way to reduce the strength of an applied electric field in electroporation is to introduce defects into cell membranes.[17,18] Vernier et al. showed, with results from both MD simulations and experiments, that the oxidation of membrane components enhanced the susceptibility of the membrane to electroporation.[19] In comparison to electroporation, sonoporation induces much less damage to cells;[3] meanwhile, it can induce water molecules inside the cell membranes.[8,9] A hybrid treatment combining

Received: July 12, 2011
Revised: September 26, 2011
Published: September 30, 2011

ultrasound with electric field could also greatly improve the poration efficiency, as indicated by a 4-fold increase in transfection level and a 6-fold increase in transfection efficiency in comparison with electroporation alone on the same cells.[20] The exciting achievement motivates us to simulate electroporation on water-containing membranes. The present simulations mimic experiments in which ultrasound treatment is carried out first and after that an external electric field is applied.

METHODS

1,2-Dioleoyl-*sn*-glycero-3-phosphoethanolamine (DOPE) bilayer membrane was adopted in the previous simulations[21] and used here again. The used simulation system included 124 DOPE lipids with CHARMM27 force field[22] and 9560 TIP3P water molecules,[23] which gave a hydration level of about 77 water molecules per lipid. After building up the water/membrane/water system, 20000-steps-energy minimization was carried out with the conjugate gradient method and followed by 8 ns relaxation at 310 K with a time step of 2 fs. Then, water molecules were randomly put into the hydrophobic region of the membrane and afterward, 500-steps-energy minimization was performed to let the simulation system reach the final state, as shown in Figure 1A. In the final setup of the simulation system, there were a total of 483 water molecules in the hydrophobic region of the membrane within -12 Å $\leq z \leq 12$ Å, where the z axis was, with its origin at the center of the membrane, perpendicular to the water/membrane interfaces. Electroporation was simulated on the final setup system under an external electric field of 0.0, 0.1, 0.2, 0.3, or 0.4 kcal/(mol·Å·e) (1 kcal/(mol·Å·e) $\approx$ 0.435 V/nm), and randomized simulations were repeated three, four, and three times for the 0.1, 0.2, and 0.3 kcal/(mol·Å·e) fields, respectively. For comparison, simulations were also performed with external electric fields of 0.4 and 0.6 kcal/(mol·Å·e) on the same membrane just after the energy minimization and relaxation without any preembedded water molecules. The 0.6 kcal/(mol·Å·e) simulations were repeated three times with each lasting for 25 ns.

The particle mesh Ewald (PME) method[24] with tinfoil boundary conditions was used to treat the long-range Coulomb interactions with the grid size smaller than 1 Å. The short-range interactions, including the van der Waals (VDW) interactions and the real-space Ewald interactions, were cut off at 12 Å with a switch function from 10 to 12 Å. The bond lengths of hydrogen atoms were constrained by the SHAKE algorithm,[25] which allows the time integration step to be 2 fs. All simulations were performed in the isothermal−isobaric (NPT) ensemble and periodic boundary conditions. The simulation temperature was set at 310 K and controlled by the Langevin dynamics. The pressure was set at 1 atm and maintained by using the Nosé−Hoover method[26] with piston fluctuations controlled by the Langevin dynamics.[27] The simulation box was allowed to change its dimensions independently along the z direction, and the x and y directions but with the same ratio of z/x and z/y. In simulations under a uniform external electric field $\mathbf{E}$, a force $\mathbf{F}_i = q_i\mathbf{E}$ was applied on every atom with partial charge q_i. The external electric field was applied along the z direction. Although there are arguments about using the tinfoil boundary conditions in the treatment of external electric field,[11] the tinfoil boundary conditions are believed to be valid if the size of the simulation cell along the direction of applied electric field is large enough.[13,28] The simulations were performed by using software NAMD2.7,[29] and software VMD[30] was adopted to visualize and analyze simulation results. The trajectories were recorded for every 1000 steps (2 ps) in all simulations.

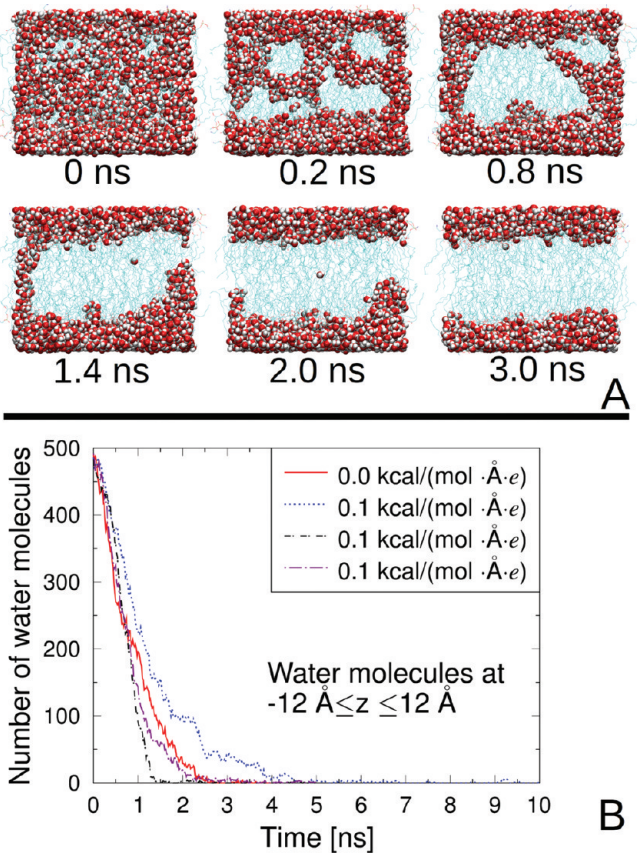

Figure 1. Water seepage dynamics in the external electric fields of 0 and 0.1 kcal/(mol·Å·e) in the water preembedded membrane. (A) Snapshots of the preembedded water molecules moving out of the hydrophobic region of membrane in the simulation without any external electric field. Water molecules are shown in the VDW representation with oxygen in red and hydrogen in white. Lipids are shown in cyan lines. Water molecules only inside and around the membrane are shown. (B) Number of water molecules in the hydrophobic region as a function of simulation time.

RESULTS AND DISCUSSION

When the external electric field was 0.0 and 0.1 kcal/(mol·Å·e), the preembedded water molecules moved out from the hydrophobic region of the membrane, as reported before.[10] Taking the case of zero electric field as an example, we showed snapshots of the process in Figure 1A, illustrating that preembedded water molecules formed small water clusters first. Then, the water clusters moved out of the membrane and the bilayer membrane became perfect. Figure 1B shows the number of water molecules within the membrane as a function of simulation time, which illustrates that water seepage dynamics in the external electric field of 0.1 kcal/(mol·Å·e) had no apparent difference from that without any electric field. The difference in the water seepage dynamics under the 0.1 kcal/(mol·Å·e) electric field observed in the three repeated simulations reflects the stochastic feature of water molecule movement and the randomized nature of MD simulations.

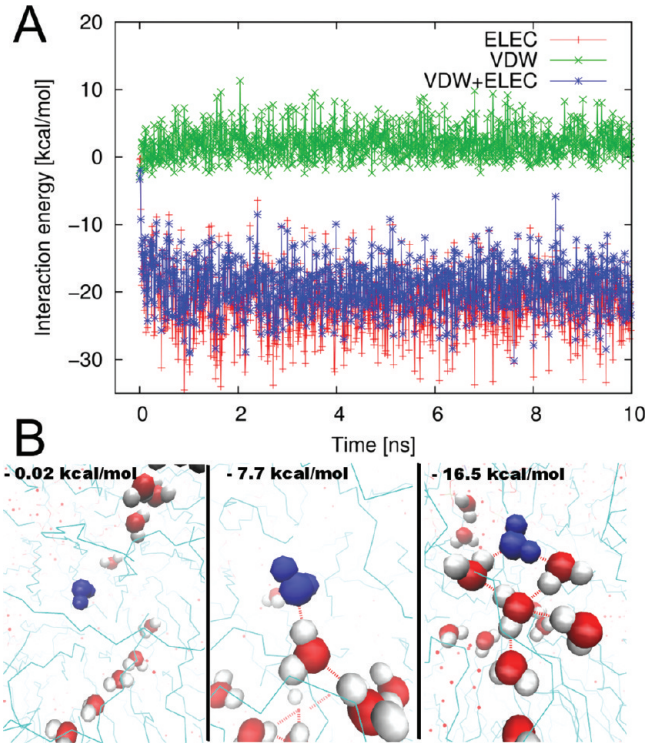

Figure 2. Interaction energies of a water molecule embedded inside the membrane with all other molecules: (A) interaction energies as a function of simulation time; (B) water molecule (blue color) initially embedded inside the membrane and its hydrogen bonds with other molecules. The electric interaction energy is −0.02 kcal/mol without any hydrogen bond, −7.7 kcal/mol with one hydrogen bond, and −16.5 kcal/mol with two hydrogen bonds. Representation scheme: oxygen of water, red balls; hydrogen of water, white balls; lipid tails: cyan lines. The water molecules within 1 nm of the specific water molecule (blue one) are shown in the VDW representation, and the hydrogen bonds are shown by dotted red lines.

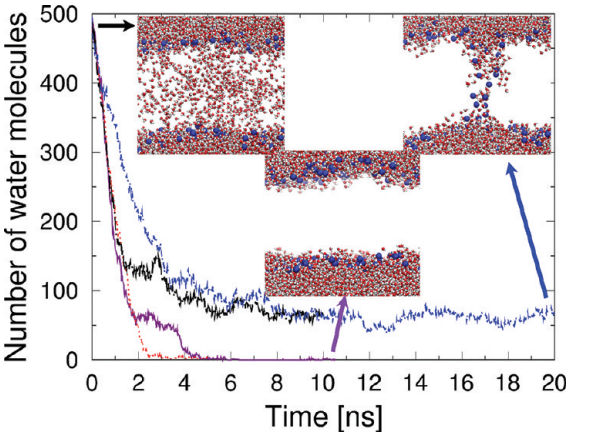

Figure 3. Water seepage dynamics in the external electric fields of 0.2 kcal/(mol·Å·e) in the water preembedded membrane. Curves show the change of number of water molecules within -12 Å $\leq z \leq$ 12 Å along time in four repeated simulations. Water molecules moved out in two simulations and stable water holes formed in another two simulations. Insets are snapshots of the initial configuration and configurations of two different results. Oxygen and hydrogen in water molecules are shown in red and white balls, respectively. Only nitrogen (blue balls) of lipids is shown to indicate the lipid headgroups and for clarity of water behaviors in membrane.

On the basis of atom coordinates and the box size information recorded in the trajectory file, the electrostatic energy and the VDW energy between a water molecule initially embedded inside the hydrophobic region of the membrane and its environment including all other water molecules and lipids were evaluated and shown in Figure 2. The electrostatic energy and the VDW energy between atoms i and j are calculated by $U_e = q_i q_j/4\pi\varepsilon_0 r_{ij}$ and $U_{VDW} = 4\varepsilon_{ij}[(\sigma_{ij}/r_{ij})^{12} - (\sigma_{ij}/r_{ij})^6]$, respectively.[29] The absolute value of the electric interaction energy is about 10−20 times larger than that of the VDW energy. In this case, it is rational to emphasize the electric energy by ignoring the VDW energy. Figure 2B shows that when the electric interaction energy is about 0 kcal/mol, no hydrogen bond is formed for the selected water molecule. A hydrogen bond is formed when the distance between two oxygen atoms in the two neighbor water molecules is smaller than 3 Å and the angle between O−H···O is larger than 120°. If one hydrogen bond is formed, the energy is reduced by about 8 kcal/mol, as shown in the second panel of Figure 2B. Due to multibody interactions, the electric energy fluctuates around −16 kcal/mol when two hydrogen bonds are formed (the third panel in Figure 2B), and the electric energy is lower than −20 kcal/mol if three and more than three hydrogen bonds are formed. For a water molecule inside bulk water, the electric interaction energy is −21.5 kcal/mol on average, meaning that one water molecule forms about three to four hydrogen bonds in bulk water. To lower the system energy, isolated water molecules inside the membrane coalesced into water clusters very quickly, as shown in Figure 2A. On the other hand, the energy cost for normal electroporation is very large, because water molecules must break some hydrogen bonds when penetrating into the membrane. When some water molecules are preembedded inside the hydrophobic region, which can be achieved by acoustic treatment, these embedded water molecules lose some hydrogen bonds already. In this case, it is much easier for electroporation to occur.

When the external electric field was 0.2 kcal/(mol·Å·e), four repeated simulations showed two different types of results (Figure 3 and movies in the Supporting Information). Two of the four repeated simulations indicated that the preembedded water molecules moved out from the membrane, similar to that observed in the 0 and 0.1 kcal/(mol·Å·e) simulations, while in another two simulations, stable water holes were held (Figure 3). In each of the two simulations, there were about 70−80 water molecules across the membrane in the stable holes. The strength of 0.2 kcal/(mol·Å·e) was approximately regarded as the minimal electric field to maintain water holes through the membrane in the simulation system. The membrane with holes had structures similar to that observed in electroporation simulations.[11−16] The external electric fields of 0.3 and 0.4 kcal/(mol·Å·e) on water preembedded membrane were also simulated three times and once, respectively. The four simulations all showed similar results on the formation of membrane-through water holes. As an example, Figure 4 showed the case for the 0.4 kcal/(mol·Å·e) field.

For the embedded-water free membrane, neither electroporation nor membrane deformation occurred in the 25 ns simulations under the 0.4 kcal/(mol·Å·e) electric field, as illustrated in Figure 5. When the external electric field was 0.6 kcal/(mol·Å·), electroporation was observed in one of the three repeated simulations (Figure 5). The other two of the three repeated simulations showed that the membrane was curved and small water

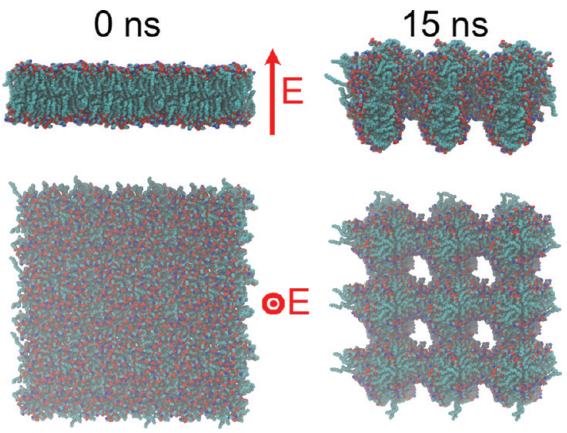

Figure 4. Snapshots of the water preembedded system in the external electric field of 0.4 kcal/(mol·Å·e). The two top pictures are the cross-section view, while the lower pictures are the top view. All lipids are shown in the VDW representation with nitrogen atoms in blue, oxygen atoms in red, and others in cyan. Water molecules are omitted for clarity. Stable water holes formed at about 10 ns and then maintained basically unchanged. The membrane patch shown is the 3 × 3 × 1 of the central simulation cell.

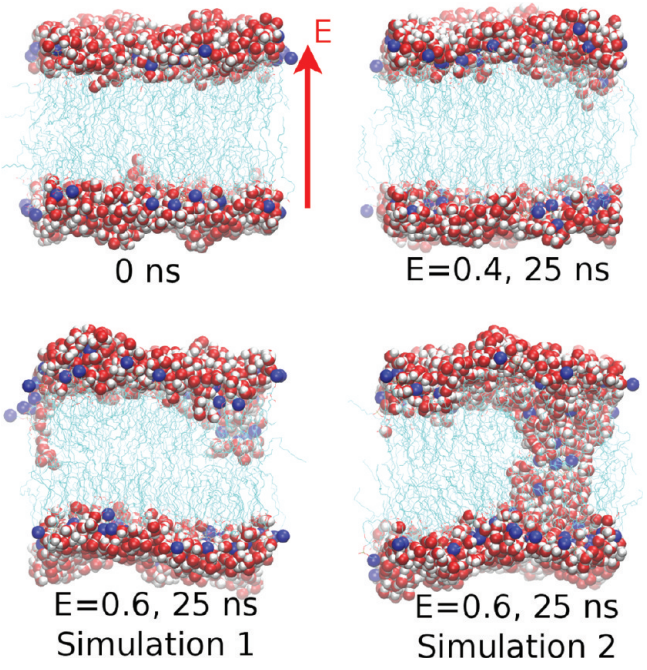

Figure 5. Snapshots of the embedded water-free system in the external electric fields of 0.4 and 0.6 kcal/(mol·Å·e). Water molecules only within 5 Å of lipids are shown for clarity. Blue balls are nitrogen atoms of lipids to indicate lipid headgroups. Lipid tails are shown in cyan lines. Water molecules are shown in the VDW presentation with oxygen in red and hydrogen in white.

clusters were formed in the hydrophobic region of the membrane. The water clusters almost went through the membrane but did not completely form the membrane-through water hole during the 25 ns simulations. One result was shown in Figure 5 as an example. Therefore, 0.6 kcal/(mol·Å·e) might be regarded as the minimal electric field for electroporation in the normal membrane based on the 25 ns cutoff time. The minimal electric field, 0.2 kcal/(mol·Å·e), to induce electroporation in water-containing membrane was much lower than 0.6 kcal/(mol·Å·e) in the same membrane without any preembedded water molecules.

Our previous simulations on electroporation of the same DOPE membrane under 1.4 kcal/(mol·Å·e) illustrated the formation of new lamellar membrane via membrane deformation and reorientation,[21] which may be responsible for cell death. The driving force of membrane rotation is the dielectric interfaces in external electric fields. When an external electric field is applied perpendicular to a dielectric interface, the interface will rotate parallel to the external electric field to minimize the electrostatic energy.[31] Such reorientation of block copolymer membranes in external electric fields was observed in both experiments[32] and simulations.[33,34] Here we checked whether membrane rotation can be also induced by a low electric field which could cause electroporation in the water-containing membrane. If the simulation was continued after the formation of stable membrane holes, the current work presented membrane deformation and rotation in the 0.3 and 0.4 kcal/(mol·Å·e) fields (movies in the Supporting Information). Increasing the external electric field to 0.4 kcal/(mol·Å·e) shortened the membrane-rotation process to about 10 ns from more than 30 ns under the external electric field of 0.3 kcal/(mol·Å·e). However, no new lamellar phase formed in the 0.3 and 0.4 kcal/(mol·Å·e) fields. Because the number of water molecules inside the membrane was limited, the system had basically a water/membrane/water lamellar structure after the membrane reorientation with water holes through the membrane. In both cases, the membrane became thicker than the original one. As an example, Figure 4 showed the case under the 0.4 kcal/(mol·Å·e) field, indicating that the simulation box shrunk along the x and y directions and stretched along the z direction. Results suggest that lower electric field can also slow membrane deformation and rotation.

CONCLUSIONS

The atomistic simulations of electroporation were conducted on the water/membrane/water system, in which water molecules were preembedded inside the hydrophobic region of membranes by acoustic treatment. The simulations demonstrate that when the applied electric field was lower than 0.2 kcal/(mol·Å·e), the embedded water molecules formed clusters and then moved out from the membrane quickly. When the applied electric field was equal to or larger than 0.2 kcal/(mol·Å·e), the embedded water molecules formed clusters and the water clusters could coalesce to stable membrane-through water holes. However, no electroporation occurred in the embedded water-free membranes after the 25 ns simulations in external electric field lower than 0.6 kcal/(mol·Å·e). The simulation results show that preacoustic treatment to embed water molecules into the hydrophobic region of membranes will greatly reduce the strength of external electric field for electroporation, which may inspire new experimental investigations.

ASSOCIATED CONTENT

Supporting Information. Movies showing two different results under the external electric field of 0.2 kcal/(mol·Å·e) and membrane deformation in the system with preembedded water under the 0.3 and 0.4 kcal/(mol·Å·e) fields. This material is available free of charge via the Internet at http://pubs.acs.org.

AUTHOR INFORMATION

Corresponding Author

*E-mail: mezhangt@ust.hk. Phone: (852) 2358-7192. Fax: (852) 2358-1543.

ACKNOWLEDGMENT

The work was partially supported by a Research Project Competition Grant, RPC06/07.SC10, from the Hong Kong University of Science and Technology (HKUST) and S.S. was partially supported by the Bioengineering Graduate Program of HKUST.

REFERENCES

(1) Chang, D. C.; Reese, T. S. *Biophys. J.* **1990**, *58*, 1–12.
(2) Zhou, Y.; Kumon, R. E.; Cui, J.; Deng, C. X. *Ultrasound Med. Biol.* **2009**, *35*, 1756–1760.
(3) Wells, D. J. *Cell Biol. Toxicol.* **2010**, *26*, 21–28.
(4) Weaver, J. C. *J. Cell. Biochem.* **1993**, *51*, 426–435.
(5) White, K. L. In *Electrofusion of mammalian cells*, 1st ed.; Nickoloff, J. A., Ed.; Humana Press: New York, 1995; Chapter 23, pp 283−294.
(6) He, H.; Chang, D. C.; Lee, Y.-K. *Bioelectrochemistry* **2007**, *70*, 363–368.
(7) Miller, D. L.; Pislaru, S. V.; Greenleaf, J. E. *Somatic Cell Mol. Genet.* **2002**, *27*, 115–134.
(8) Koshiyama, K.; Kodama, T.; Yano, T.; Fujikawa, S. *Biophys. J.* **2006**, *91*, 2198–2205.
(9) Koshiyama, K.; Kodama, T.; Yano, T.; Fujikawa, S. *Biochim. Biophys. Acta* **2008**, *1778*, 1423–1428.
(10) Koshiyama, K.; Yano, T. *Phys. Rev. Lett.* **2010**, *105*, No. 018105.
(11) Böckmann, R. A.; de Groot, B. L.; Kakorin, S.; Neumann, E.; Grubmüller, H. *Biophys. J.* **2008**, *95*, 1837–1850.
(12) Tarek, M. *Biophys. J.* **2005**, *88*, 4045–4053.
(13) Tieleman, D. P. *BMC Biochem.* **2004**, *5*, No. 10.
(14) Tieleman, D. P.; Leontiadou, H.; Mark, A. E.; Marrink, S. J. *J. Am. Chem. Soc.* **2003**, *125*, 6382–6383.
(15) Vernier, P. T.; Ziegler, M. J. *J. Phys. Chem. B* **2007**, *111*, 12993–12996.
(16) Ziegler, M. J.; Vernier, P. T. *J. Phys. Chem. B* **2008**, *112*, 13588–13596.
(17) Marrink, S. J.; de Vries, A. H.; Tieleman, D. P. *Biochim. Biophys. Acta* **2009**, *1788*, 149–168.
(18) Gurtovenko, A. A.; Anwar, J.; Vattulainen, I. *Chem. Rev.* **2010**, *110*, 6077–6103.
(19) Vernier, P. T.; Levine, Z. A.; Wu, Y.-H.; Joubert, V.; Ziegler, M. J.; Mir, L. M.; Tieleman, D. P. *PloS One* **2009**, *4*, No. e7966.
(20) Escoffre, J. M.; Kaddur, K.; Rols, M. P.; Bouakaz, A. *Ultrasound Med. Biol.* **2010**, *36*, 1746–1755.
(21) Sun, S.; Wong, J. T. Y.; Zhang, T.-Y. *Soft Matter* **2011**, *7*, 147–152.
(22) Feller, S. E.; MacKerell, A. D. *J. Phys. Chem. B* **2000**, *104*, 7510–7515.
(23) Jorgensen, W.; Chandrasekhar, J.; Madura, J.; Impey, R.; Klein, M. *J. Chem. Phys.* **1983**, *79*, 926–935.
(24) Essmann, U.; Perera, L.; Berkowitz, M. L.; Darden, T.; Lee, H.; Pedersen, L. G. *J. Chem. Phys.* **1995**, *103*, 8577–8593.
(25) Ryckaert, J.; Ciccotti, G.; Berendsen, H. *J. Comput. Phys.* **1977**, *23*, 327–341.
(26) Martyna, G. J.; Tobias, D. J.; Klein, M. L. *J. Chem. Phys.* **1994**, *101*, 4177–4189.
(27) Feller, S. E.; Zhang, Y.; Pastor, R. W.; Brooks, B. R. *J. Chem. Phys.* **1995**, *103*, 4613–4621.
(28) Roux, B. *Biophys. J.* **2008**, *95*, 4205–4216.
(29) Phillips, J. C.; Braun, R.; Wang, W.; Gumbart, J.; Tajkhorshid, E.; Villa, E.; Chipot, C.; Skeel, R. D.; Kalé, L.; Schulten, K. *J. Comput. Chem.* **2005**, *26*, 1781–1802.
(30) Humphrey, W. *J. Mol. Graph.* **1996**, *14*, 33–38.
(31) Tsori, Y. *Rev. Mod. Phys.* **2009**, *81*, 1471–1494.
(32) Böker, A.; Elbs, H.; Hänsel, H.; Knoll, A.; Ludwigs, S.; Zettl, H.; Urban, V.; Abetz, V.; Müller, A.; Krausch, G. *Phys. Rev. Lett.* **2002**, *89*, 1–4.
(33) Kyrylyuk, A. V.; Zvelindovsky, A. V.; Sevink, G. J. A.; Fraaije, J. G. E. M. *Macromolecules* **2002**, *35*, 1473–1476.
(34) Pinna, M.; Schreier, L.; Zvelindovsky, A. V. *Soft Matter* **2009**, *5*, 970–973.